Anomalous Nernst and anisotropic magnetoresistive heating in a lateral spin valve

Slachter, Abraham; Bakker, Frank Lennart; van Wees, Bart Jan

Published in:
Physical Review. B: Condensed Matter and Materials Physics

DOI:
10.1103/PhysRevB.84.020412

Publication date:
2011

PHYSICAL REVIEW B **84**, 020412(R) (2011)

Anomalous Nernst and anisotropic magnetoresistive heating in a lateral spin valve

Abraham Slachter,* Frank Lennart Bakker, and Bart Jan van Wees
Physics of Nanodevices, Zernike Institute for Advanced Materials, University of Groningen, Groningen, The Netherlands
(Received 16 March 2011; revised manuscript received 26 May 2011; published 22 July 2011)

We measured the anomalous Nernst effect and anisotropic magnetoresistive heating in a lateral multiterminal permalloy/copper spin valve using all-electrical lock-in measurements. To interpret the results, a three-dimensional thermoelectric finite-element model is developed. Using this model, we extract the heat profile which we use to determine the anomalous Nernst coefficient of permalloy $R_N = 0.13$ and also determine the maximum angle $\theta = 8^\circ$ of the magnetization prior to the switching process when an opposing noncollinear 10° magnetic field is applied.

DOI: 10.1103/PhysRevB.84.020412 PACS number(s): 85.75.−d, 72.15.Jf, 72.25.−b, 85.80.−b

The connection between thermoelectricity and spintronics[1] has recently attracted much attention,[2–5] which led to the subfield called spin caloritronics.[6] Although thermoelectric effects are typically regarded to be small, we have recently shown that they can be dominant in lateral multiterminal devices such as nonlocal spin valves.[5,7] Here we demonstrate two thermal effects which can accompany such functionality in nanoscale spin-caloritronic devices: the anomalous Nernst effect and anisotropic magnetoresistive heating. We show that both effects can dominate the thermoelectric behavior and can be modeled accurately.

The anomalous Nernst effect can be interpreted as the thermoelectric equivalent of the anomalous Hall effect.[8,9] When a temperature gradient is applied to a ferromagnet, a voltage gradient perpendicular to the plane made by the magnetization and temperature gradient develops and vice versa. Both effects are related to each other and are described by the same Nernst coefficient R_N. The first effect is governed by the following equation:

$$\vec{\nabla} V_N = -S_N \vec{m} \times \vec{\nabla} T. \tag{1}$$

Here $\vec{m}$ is the unit vector pointing in the magnetization direction, T is the temperature, and $\vec{\nabla} V_N$ is the resulting voltage gradient due to anomalous Nernst effect. $S_N = R_N S$ is the transverse Seebeck coefficient representing the strength of the effect, which is a fraction of the Seebeck coefficient S.

The anisotropic magnetoresistance (AMR) describes how the resistance of a ferromagnet changes with respect to the angle θ between the magnetization and the current direction. The conductivity of the ferromagnet is given by $\sigma_{\mathrm{FM}} = \sigma_{\parallel}\{1 + R_{\mathrm{AMR}}[\cos^2(\theta) - 1]\}$, where $\sigma_{\parallel}$ is the conductivity measured when the direction of the current is parallel to the magnetization and R_{AMR} is a small fraction. When a current is sent through a ferromagnet, the Joule heating of this ferromagnet depends on the resistance of the magnet. Therefore, the Joule heating of a ferromagnet depends on the angle between the magnetization and the direction of the current. Because the nonlocal voltages measured in a lateral multiterminal device depend on the generated heat,[7] this angle can be deduced from measurements. We refer to this effect as AMR heating.

To demonstrate both effects, we fabricated a multiterminal lateral spin valve. This device is shown in Fig. 1. It consists of two permalloy ($Ni_{80}Fe_{20}$) ferromagnets connected by a highly conductive copper strip. The first ferromagnet FM_1 is provided with three thick highly thermally conductive Ti/Au contacts which allows to locally heat this ferromagnet by sending currents through it. The generated heat is transported to the second ferromagnet FM_2 by the thermally conductive copper strip. This heat can be detected by measuring the temperature of this ferromagnet close to the Py/Cu interface. We do this by providing two thermocouples to FM_2. The outer sides are thermally anchored by two gold contacts, while close to the interface two NiChrome ($Ni_{80}Cr_{20}$) contacts are present. Due to the opposite Seebeck coefficients of permalloy ($S = -20\ \mu$V/K) and NiChrome ($S = 20\ \mu$V/K) both thermocouples (contact 4–5 and 6–7) have a thermal sensitivity of $S_{\text{Py-NiCr}} \approx 40\ \mu$V/K and effectively measure the temperature of the magnet under the Nichrome contacts.

The device was fabricated in a one-step optical and six-step electron beam lithography. First, large 5/150-nm-thick Ti/Au contacts are made using an optical lithography step and electron beam deposition, after which 100-nm-wide and 5/30-nm-thick Ti/Au markers are fabricated using electron beam lithography. In subsequent lithography steps, 15-nm-thick permalloy, a 5/30-nm-thick Ti/Au interlayer, 5/170-nm-thick Ti/Au, 45-nm NiCr, and 60-nm copper were deposited using electron beam deposition.

In our experiment, we selectively switch the magnetizations of both magnets FM_1 and FM_2 by applying an antiparallel magnetic field and observe the heat transported through the spin valve by Joule heating FM_1 and measuring the voltage of the thermocouples on FM_2. Since the Joule heating scales with I^2, we are only interested in the R_2 (μV/mA^2) component of the measured voltage $V = R_1 I + R_2 I^2 \cdots$, which we determine by performing lock-in measurements.[5,7] All measurements were done at room temperature.

How exactly the anomalous Nernst effect and AMR heating can be measured in this device is illustrated in Fig. 2. The generated heat in the device is transported by the four contacts making up the two thermocouples. At the NiCr contacts the heat is transported in the plane of the device, while at the gold contacts this predominantly takes place perpendicular to the plane of the device owing to the difference in thermal conductivity between the materials. The asymmetry and three-dimensional nature of the contacts assures that part of the generated anomalous Nernst voltage differences result in a small voltage difference between the contacts. The sign of this

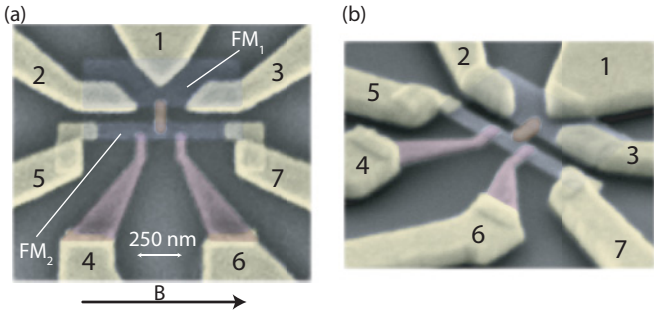

FIG. 1. (Color online) Colored scanning electron microscope images of the fabricated device. (a) Top view of the device. The two ferromagnets are connected to each other by a copper strip. FM_1 is connected by three thick gold heat sinks (1–3) through which we can send a charge current to heat it. FM_2 is also connected by two gold heat sinks (5,7), but have two additional NiChrome contacts (4,6). The magnetizations $\vec{M}_1$ and $\vec{M}_2$ are selectively switched by applying an opposing magnetic field $\vec{B}$. (b) Three-dimensional image of the device illustrating the thick gold contact used as thermal heat sinks.

voltage difference changes when the magnetization direction M_2 flips.

In the same device there are three contacts connected to FM_1 to send the current either aligned parallel to the magnetization direction (I_{2-3}) or under a $\pm 45^\circ$ angle (I_{1-2} or I_{1-3}). When the opposing magnetic field in a spin valve has a small angle with respect to the antiparallel direction of the magnetization M_1, the magnetization rotates prior to the switching process, which either increases or decrease the Joule heating. This effect should be pronounced when the current is send under a $\pm 45^\circ$

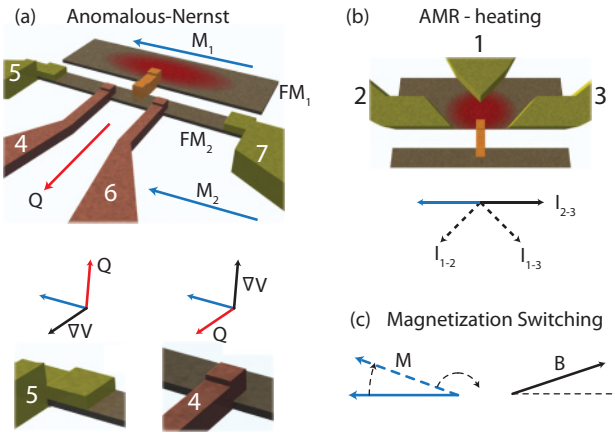

FIG. 2. (Color online) Illustration of the anomalous Nernst effect and magnetoresistive heating. (a) The Joule heating of FM_1 induces a heat flow Q through FM_2 and the four contacts connecting it. The anomalous Nernst effect induces voltage gradients in the ferromagnet perpendicular to the heat flow and magnetization M_2. (b) Three contacts are present on FM_1 to send the current parallel or under a $\pm 45^\circ$ angle with respect to the magnetization of FM_1. (c) When the opposing magnetic field has a small angle with respect to the antiparallel direction of the magnetization, the magnetization first rotates prior to switching at its switching field, increasing or decreasing the Joule heating depending on the orientation of the current.

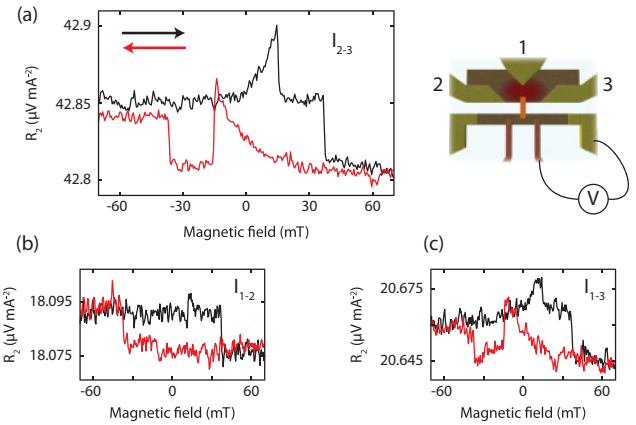

FIG. 3. (Color online) Measured voltage from the Py-NiCr thermocouple by selectively switching the magnetizations by an antiparallel magnetic field in a lateral spin valve. The right-hand thermocouple is measured when the Joule heating current is sent (a) parallel to the magnetization M_1, (b) under a 45° angle and (c) under a -45° angle. The results were calculated by sending a rms charge current of 1.5 mA. The other thermocouple was also measured and shows similar results.

angle as the change in conductance is then linearly dependent on this deviation angle of the magnetization with the easy axis, while in the parallel case this depends quadratically on this angle.

The measured nonlinear voltage R_2 (μV/mA^2) from the thermocouples is shown for different orientations of the currents in Fig. 3. Owing to the different dimensions of the ferromagnets, FM_1 switches by an antiparallel magnetic field of $\sim$15 mT while FM_2 switches at $\sim$40 mT. We observe a clear change in the voltage at the switching field of FM_2. We see this voltage depends only on the orientation of the magnetization of FM_2. Owing to the finite field at which this magnetization changes sign, the measurement shows a hysteresis loop. When the current is sent parallel to the magnetization, a voltage of 37 nV/mA^2 can be measured depending on the orientation of M_2 on top of a large 42.83 μV/mA^2 background originating from the temperature measured by the Py-NiCr thermocouple. When the current is sent under a 45° angle we measure a smaller 18 nV/mA^2 signal on top of a smaller 18.085 and 20.65 μV/mA^2 background owing to the smaller current path which reduces the Joule heating. We note that the switches do not depend on the thermocouple we measured.

In addition, we see a feature appearing prior to the switching of FM_1 which is different in size depending on the current direction. We believe this can be attributed to AMR heating. To confirm this, we performed our measurements using a magnetic field 10° clockwise or anticlockwise to the antiparallel of the magnetizations for the $\pm 45^\circ$ angles between the current we sent through FM_1 and the magnetization axis. The results of these measurements are shown in Fig. 4.

We clearly observe that the AMR heating increases or decreases by rotating the magnetization prior to switching and has the correct symmetry for a ferromagnetic resistance which is higher for the parallel alignment of the magnetization and current. The voltages arising from this effect are up to

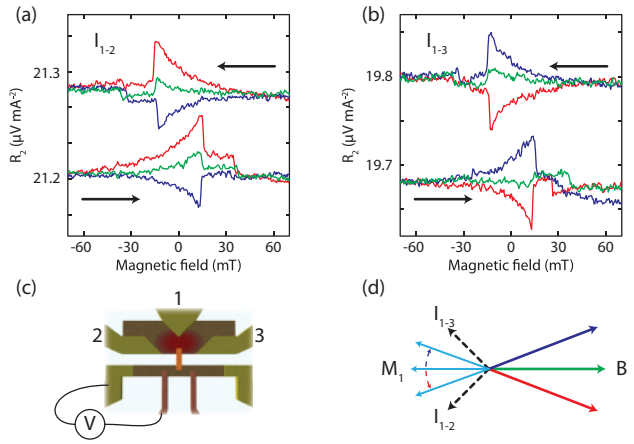

FIG. 4. (Color online) Measured voltage from the Py-NiCr thermocouple by selectively switching the magnetizations by an opposing magnetic field at 0° and ±10°. The left-hand thermocouple is measured when (a) sending the current under a 45° angle and (b) under a −45° angle with respect to the easy magnetization axis. (c) The measured configuration and (d) the magnetic field configuration and current direction for the measurements of (a) and (b). The other thermocouple was also measured and shows similar results.

50 nV/mA^2 in magnitude on top of a 19.7 and 21.1 μV/mA^2 background, showing that this effect increases or decreases the heating measured by the thermocouple by ∼0.25%. The small remaining feature appearing at 0° for the experiment in Fig. 3 is attributed to the imperfect alignment of the magnetic field in our experiment. We also note that, owing to the high conductivity of gold contact 1, the current path does not go exactly straight through the ferromagnet when the current is sent from contact 2 to contact 3. The current path is slightly short circuited, which leads to a significant component of the current path which is noncollinear to the magnetization. This effect can be seen by the strong anisotropic magnetoresistive heating component of Fig. 3(a).

In order to quantify the size of the anomalous Nernst effect and AMR heating, we extend the thermoelectric model used in Ref. 7 to include these effects. We use a set of differential equations given by the conservation of charge and heat currents:

$$\begin{pmatrix} \vec{J} \\ \vec{Q} \end{pmatrix} = -\begin{pmatrix} \sigma & \sigma S \\ \sigma \Pi & k \end{pmatrix} \begin{pmatrix} \vec{\nabla} V \\ \vec{\nabla} T \end{pmatrix}, \tag{2}$$

where $\vec{J}$ and $\vec{Q}$ are the charge and heat currents which are related to the voltage gradient $\vec{\nabla} V$ and temperature gradient $\vec{\nabla} T$ by the electrical conductivity σ, thermal conductivity k, Seebeck coefficient S, and Peltier coefficient $\Pi = ST_0$, with $T_0 = 293.15$ K the reference temperature of the device. The conservation of these currents is given by $\vec{\nabla} \cdot \vec{J} = 0$ and $\vec{\nabla} \cdot \vec{Q} = \vec{J} \cdot \vec{J}/\sigma$, where we have included Joule heating by the net charge current $\vec{J}$ as defined in Eq. (2). In this model, spin-dependent thermoelectric transport[5] or Joule heating[12] is excluded since any effects arising from the coupling of spin and heat are negligible. The model introduced in Ref. 7 is an isotropic model with isotropic coefficients σ, k, and S. We include AMR and the anomalous Nernst effect by adding anisotropic components to σ and S, respectively.

AMR for the magnetization pointing in the direction of any of the three principle axis can be included by using a diagonal 3 × 3 conductivity matrix σ, with $\sigma_\parallel$ on one element of the diagonal and $\sigma_\perp$ on the other elements. When the magnetization points in an arbitrary direction given by the angles θ and ϕ, this diagonal matrix rotates by $\mathbf{R}\,\sigma\,\mathbf{R}^{-1}$, where $\mathbf{R}$ is the rotation matrix which rotates the $(\parallel, \perp_1, \perp_2)$ axes to the (x, y, z) axes. This matrix then becomes

$$\sigma_{ij} = \sigma_\perp(\delta_{ij} - R_{\mathrm{AMR}} m_i m_j), \tag{3}$$

where $i, j = x, y, z$, m_i are the x, y, z components of the unit vector $\vec{m}$ pointing in the direction of the magnetization, and δ_{ij} is the Kronecker delta.

We include the anomalous Nernst effect by including Eq. (1) into the currents defined in Eq. (2). The Seebeck coefficient S now becomes a skew symmetric matrix $\mathbf{S}$ given by

$$\mathbf{S}_{ij} = S\left(\delta_{ij} - R_N \sum_k \varepsilon_{ijk} m_k\right), \tag{4}$$

where ε_{ijk} is the Levi-Civita symbol. A top view of the three-dimensional geometry used for the finite-element model is shown in Fig. 5. We included a piece of 2.2 × 3 μm of the device and set the temperature at all electrical contacts to T_0. All other outer contact areas are electrically and thermally isolating, while on the inner contacts we take the heat and charge current to be continuous. A charge current is sent through the device by putting a charge current boundary condition on contact 2 and the voltage $V = 0$ on contacts 1 or 3. The parameters in Fig. 5(b) were used to calculate the temperature rise of the device and subsequent voltage measured by the thermocouples. The 300-nm-thick silicon oxide substrate is also modeled, as well as 700 nm of highly thermally conductive n-doped silicon.[11]

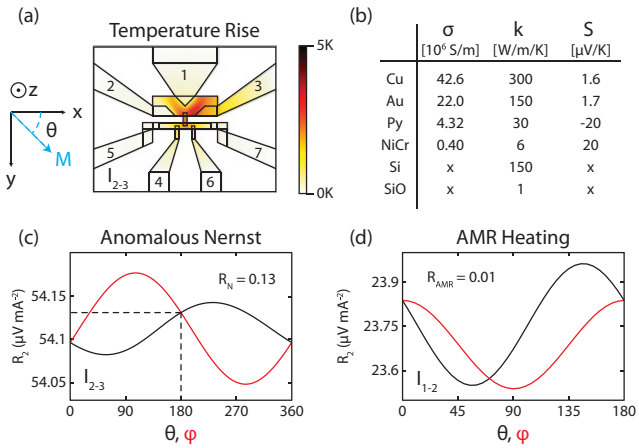

	σ [10^6 S/m]	k [W/m/K]	S [μV/K]
Cu	42.6	300	1.6
Au	22.0	150	1.7
Py	4.32	30	-20
NiCr	0.40	6	20
Si	x	150	x
SiO	x	1	x

FIG. 5. (Color online) Simulated results of the three-dimensional thermoelectric model. (a) The temperature distribution of the device with a current of 1 mA sent parallel (I_{2-3}) to the alignment of the magnetization. (b) Input parameters used for the model. The electrical conductivities σ are measured while the others are taken from literature (Refs. 10 and 11). (c) The simulated anomalous Nernst voltage from the thermocouples 4–5 and 6–7 as a function of the magnetization angles θ on the x-y axis and ϕ between the x-y plane and the z axis of FM_2. (d) The simulated AMR heating as a function of the magnetization direction of FM_1.

We first excluded AMR and the anomalous Nernst effect in our model and calculated the voltages arising at our thermocouples. We calculate this for the measurement geometries shown in Figs. 3(a)–3(c). A background of, respectively, $R_2 = 54.11\ \mu\mathrm{V/mA^2}$, $R_2 = 23.99\ \mu\mathrm{V/mA^2}$, and $R_2 = 26.07\ \mu\mathrm{V/mA^2}$ was calculated for these three geometries, which is ∼25% higher than observed. This small discrepancy is attributed to the precision of the parameters used.

In the following, we calculate the contribution from the anomalous Nernst effect to this background voltage. We focus on the measurement geometry and result given in Fig. 3(a). Figure 5(b) shows the calculated voltage as a function of the FM_2 magnetization angles θ in the x-y plane and ϕ perpendicular to the plane. We find that an anomalous Nernst coefficient of $R_N = 0.13$ accurately predicts the 37-nV voltage observed depending on the magnetization direction pointing along the easy axis of FM_2. The size of the anomalous Nernst effect is most sensitive to the out-of-plane angle ϕ because the heat currents are predominantly pointing in the plane of the device. Nevertheless, a finite voltage is expected, which is approximately one third of the maximum effect calculated for an out-of-plane magnetization at $\phi = 105^\circ$ and $\phi = 285^\circ$. Using the Seebeck coefficient of permalloy $S_{\mathrm{Py}} = -20\ \mu\mathrm{V/K}$,[2] this leads to a transverse Seebeck coefficient of $S_N = -2.6\ \mu\mathrm{V/K}$.

The size of this coefficient should be equal to that of the anomalous Hall coefficient when the semiclassical band model applies.[9] This relates these coefficients by the Mott formula for thermoelectricity. We find that it is somewhat larger then the typical anomalous Hall coefficient of ferromagnetic metals[8] of 10^{-2}. However, permalloy is also approximately ten times less conductive then the ordinary ferromagnetic metals. When we take this into account, and also the measured size of the anomalous Hall coefficient of permalloy,[13] we find that our results are in agreement with a semiclassical band model.

The AMR heating is calculated for varying angles θ and ϕ of the magnetization of FM_1 for the measurement geometry used in Fig. 4. We use an AMR coefficient $R_{\mathrm{AMR}} = 0.01$ determined from previous experiments.[14] The result is shown in Fig. 5(d). The calculated voltage from the thermocouple varies by as much as $400\ \mathrm{nV/mA^2}$ when the magnetization points at $\theta = 60^\circ$ or $\theta = 145^\circ$. In our experiments we find that when an opposing magnetic field with a $\pm 10^\circ$ with respect to the magnetization axis is applied, the voltage prior the switch of the magnetization is ≈50 nV. From the calculations we determine that this corresponds to a deviation of the magnetization angle of FM_1 with the easy axis of 8°.

In conclusion, we have demonstrated how anisotropic magnetoresistive heating and the anomalous Nernst effect can be measured in a dedicated caloritronic device. We used a three-dimensional finite-element model which includes charge and heat transport to model these effects. We extracted an anomalous Nernst coefficient of $R_N = 0.13$ for permalloy and found that the magnetization of a permalloy nanoscale magnet tilts ∼7°–8° before switching when an opposing magnetic field at a 10° angle to the easy axis is applied.

We would like to acknowledge B. Wolfs, S. Bakker, and J.G. Holstein for technical assistance. This work was financed by the European EC Contracts IST-033749 "DynaMax," the "Stichting voor Fundamenteel Onderzoek der Materie" (FOM), and NanoNed.

*a.slachter@gmail.com

[1] I. Zutic, J. Fabian, and S. Das Sarma, Rev. Mod. Phys. **76**, 323 (2004).

[2] K. Uchida, S. Takahashi, K. Harii, J. Ieda, W. Koshibae, K. Ando, S. Maekawa, and E. Saitoh, Nature (London) **455**, 778 (2008).

[3] K. Uchida, J. Xiao, H. Adachi, J. Ohe, S. Takahashi, J. Ieda, T. Ota, Y. Kajiware, H. Umezawa, H. Kawai, G. E. W. Bauer, S. Maekawa, and E. Saitoh, Nature (London) **9**, 894 (2010).

[4] N. Liebing, S. Serrano-Guisan, G. Reiss, J. Langer, B. Ocker, and H. W. Schumacher, e-print arXiv:1104.0537v2.

[5] A. Slachter, F. L. Bakker, J-P. Adam, and B. J. van Wees, Nat. Phys. **6**, 879 (2010).

[6] G. E. W. Bauer, A. H. MacDonald, and S. Maekawa, Solid State Commun. **150**, 459 (2010).

[7] F. L. Bakker, A. Slachter, J.-P. Adam, and B. J. van Wees, Phys. Rev. Lett. **105**, 136601 (2010).

[8] N. Nagaosa, J. Sinova, S. Onoda, A. H. MacDonald, and N. P. Ong, Rev. Mod. Phys. **82**, 1539 (2010).

[9] K. Behnia, J. Phys. Condens. Matter **21**, 113101 (2009).

[10] C. Kittel, *Introduction to Solid State Physics* (Wiley, New York, 1995).

[11] J. Thompson and B. A. Younglove, J. Phys. Chem. Solids **20**, 146 (1961).

[12] A. A. Tulapurkar and Y. Suzuki, Phys. Rev. B **83**, 012401 (2011).

[13] J. Smit, Physica **21**, 877 (1955).

[14] M. V. Costache, M. Sladkov, S. M. Watts, C. H. van der Wal, and B. J. van Wees, Phys. Rev. Lett. **97**, 216603 (2006).